J|A|C|S ARTICLES

Published on Web 03/12/2010

Gold Nanoparticles for the Improved Anticancer Drug Delivery of the Active Component of Oxaliplatin

Sarah D. Brown,[†,‡] Paola Nativo,[†] Jo-Ann Smith,[‡] David Stirling,[§] Paul R. Edwards,[||] Balaji Venugopal,[⊥] David J. Flint,[‡] Jane A. Plumb,[⊥] Duncan Graham,*[,†] and Nial J. Wheate*[,‡]

Centre for Molecular Nanometrology, Department of Pure and Applied Chemistry, Thomas Graham Building, University of Strathclyde, 295 Cathedral Street, G1 1XL Glasgow, United Kingdom, Strathclyde Institute of Pharmacy and Biomedical Sciences, University of Strathclyde, 27 Taylor Street, G4 0NR Glasgow, United Kingdom, School of Engineering and Science, University of the West of Scotland, Paisley Campus, High Street Paisley, PA1 2BE United Kingdom, Department of Physics, John Anderson Building, University of Strathclyde, 107 Rottenrow, G4 0NG, Glasgow, United Kingdom, and Centre for Oncology and Applied Pharmacology, University of Glasgow, Cancer Research UK Beatson Laboratories, Garscube Estate, G61 1BD Glasgow, United Kingdom

Received September 25, 2009; E-mail: duncan.graham@strath.ac.uk; nial.wheate@strath.ac.uk

Abstract: The platinum-based anticancer drugs cisplatin, carboplatin, and oxaliplatin are an important component of chemotherapy but are limited by severe dose-limiting side effects and the ability of tumors to develop resistance rapidly. These drugs can be improved through the use of drug-delivery vehicles that are able to target cancers passively or actively. In this study, we have tethered the active component of the anticancer drug oxaliplatin to a gold nanoparticle for improved drug delivery. Naked gold nanoparticles were functionalized with a thiolated poly(ethylene glycol) (PEG) monolayer capped with a carboxylate group. [Pt(1*R*,2*R*-diaminocyclohexane)(H_2O)$_2$]2NO_3 was added to the PEG surface to yield a supramolecular complex with 280 (±20) drug molecules per nanoparticle. The platinum-tethered nanoparticles were examined for cytotoxicity, drug uptake, and localization in the A549 lung epithelial cancer cell line and the colon cancer cell lines HCT116, HCT15, HT29, and RKO. The platinum-tethered nanoparticles demonstrated as good as, or significantly better, cytotoxicity than oxaliplatin alone in all of the cell lines and an unusual ability to penetrate the nucleus in the lung cancer cells.

Introduction

Since its approval in 1971, cisplatin has been used to treat a variety of human cancers.[1] Whereas the drug has a nearly 100% cure rate for testicular cancer, its use in treating ovarian, bladder, lung, head, and neck cancers is limited by acquired resistance. Cisplatin and its analogues carboplatin and oxaliplatin act by binding to DNA, thereby preventing its transcription and replication and through that inducing cellular apoptosis.[2,3] Resistance can arise from reduced drug uptake/enhanced efflux, increased repair/tolerance of drug−DNA adducts, and increased intracellular levels of the tripeptide glutathione that can readily degrade and deactivate cisplatin.[1] Recently, elevated intracellular chloride concentrations have been shown to be another possible mechanism of resistance.[4] The use of cisplatin is also limited because of its severe dose-limiting side effects that include nephrotoxicity, ototoxicity, and neurotoxicity.[1] In the past decade, only one new platinum drug, oxaliplatin, has been approved worldwide, and although it has shown potential for treating a range of cancers, it is only currently used for colorectal tumors. Like cisplatin, the use of oxaliplatin is limited by neurotoxicity, nausea, and vomiting.[1]

Many of the side effects of cisplatin and oxaliplatin are due to their nonspecific attack of all rapidly dividing cells; therefore, platinum-based chemotherapy can be greatly improved through enhanced drug delivery. Platinum drugs can be passively targeted to solid tumors through the enhanced permeability and retention effect.[5] Alternatively, platinum drugs can be actively targeted to both solid tumors and leukemias through the use of aptamers,[6] peptides,[7] antibodies,[8] or cancer-related substrates (such as folate).[9]

Over the past decade, gold nanoparticles have been developed that demonstrate a wide variety of applications, including

[†] Centre for Molecular Nanometrology, University of Strathclyde.
[‡] Strathclyde Institute of Pharmacy and Biomedical Sciences, University of Strathclyde.
[§] University of the West of Scotland.
[||] Department of Physics, University of Strathclyde.
[⊥] University of Glasgow.

(1) Kelland, L. *Nat. Rev. Cancer* **2007**, *7*, 573.
(2) Todd, R. C.; Lippard, S. J. *Metallomics* **2009**, *1*, 280.
(3) Wang, D.; Lippard, S. J. *Nat. Rev. Drug Discovery* **2005**, *4*, 307.
(4) Salerno, M.; Yahia, D.; Dzamitika, S.; de Vries, E.; Pereira-Maia, E.; Garnier-Suillerot, A. *J. Biol. Inorg. Chem.* **2009**, *14*, 123.
(5) Kratz, F.; Müller, I. A.; Ryppa, C.; Warnecke, A. *ChemMedChem* **2008**, *3*, 20.
(6) Farokhzad, O. C.; Jon, S.; Khademhosseini, A.; Tran, T.-N. T.; LaVan, D. A.; Langer, R. *Cancer Res.* **2004**, *64*, 7668.
(7) Dharap, S. S.; Wang, Y.; Chandna, P.; Khandare, J. J.; Qiu, B.; Gunaseelan, S.; Sinko, P. J.; Stein, S.; Farmanfarmaian, A.; Minko, T. *Proc. Natl. Acad. Sci. U.S.A* **2005**, *102*, 12962.
(8) Cheng, W. W. K.; Allen, T. M. *J. Controlled Release* **2008**, *126*, 50.
(9) Kelemen, L. E. *Int. J. Cancer* **2006**, *119*, 243.

 10.1021/ja908117a

catalysis,[10] bioanalysis, and imaging.[11,12] Gold nanoparticles are also an ideal drug-delivery scaffold because they are known to be nontoxic and nonimmunogenic.[13,14] Gold nanoparticles can also be readily functionalized with multiple targeting molecules and have so far shown excellent potential for the delivery of other nonplatinum-based drugs[15−18] and a platinum(IV) complex.[19] Several gold nanoparticle-based drugs are currently under development by CytImmune, with their lead drug, Aurimune, in clinical trials.[20] The size of the gold nanoparticles can also be controlled. Typically, gold nanoparticles ranging from 13 to 60 nm can be easily made by a simple reduction of the gold salts in water[21−23] or by starting with seed particles of 13 to 20 nm followed by a second reduction step involving more gold salt.[24−26] As such, gold nanoparticles with very high surface areas suitable for the attachment of a large number of platinum drug molecules are readily available.

In this article, we report the synthesis of a platinum-tethered gold nanoparticle for improved anticancer drug delivery, where the platinum molecule is the active component of oxaliplatin: [Pt(1*R*,2*R*-diaminocyclohexane]$^{2+}$ ([Pt(dach]). This was characterized using dynamic light scattering, scanning electron microscopy, electron probe microanalysis, and inductively coupled plasma mass spectrometry (ICP-MS). Its in vitro uptake, localization, and cytotoxicity in A549 lung and HCT116, HCT15, HT29, and RKO colon cancer cells was also examined using growth inhibition assays, ICP-MS, and transmission electron microscopy.

Experimental Section

Mass Spectrometry. Nanoparticles (900 μL, 26.7 nM based on the extinction coefficient of gold) were digested using NaCN solution (100 μL, 0.067 M) for 24 h and then analyzed on a Thermo Electron Corp. X-Series II quadrupole ICP-MS. The instrument used a concentric nebulizer with a Peltier-cooled conical single-pass spray chamber with impact bead and an integral peristaltic pump for sample uptake from a Cetac ASX-520 autosampler. A hexapole for CCT ED (collision cell technology with energy discrimination) mode was used to remove polyatomic interference. The instrumental operating conditions were 1400 W rf forward power, 13 L min^{-1} plasma flow, 1.0 L min^{-1} nebulizer flow, and 0.8 L min^{-1} auxiliary flow. A sample flush time of 60 s, a wash time of 60 s, and a peak jump mode were used with a dwell time per isotope of 10 ms. Pt was determined using the ^{194}Pt and ^{195}Pt isotopes. Calibration solutions were prepared from a Spex "CertiPrep" certified standard diluted as required with 2% Fisher "Primar Plus" nitric acid.

Scanning Electron Microscopy. Samples of naked nanoparticle, PEGylated nanoparticles, and platinum-tethered nanoparticle (1 μL) were dried on a silicon substrate and placed under vacuum. SEM images were collected using a FEI Sirion 200 ultrahigh-resolution Schottky field-emission scanning electron microscope running FEI software. An accelerating voltage of 5 kV was applied to each sample, and a spot size of 3 was used.

Electron Probe Microanalyser (EPMA). A sample of platinum-tethered nanoparticle (1 μL) was dried on a silicon substrate and placed under vacuum. The wavelength-dispersive X-ray spectrum was acquired in a Cameca SX100 electron probe microanalyzer using a pentaerythritol crystal with a lattice spacing of $2d = 8.75$ Å at 20 keV, and a 40 nA electron beam was used.

Dynamic Light Scattering. Dynamic light scattering and zeta potential experiments were conducted on a Malvern Zetasizer Nano ZS. The machine was calibrated using a 60 nm polystyrene standard. Each 5 nM, 1 mL sample was loaded into a cell, and the particle size and zeta potential were measured simultaneously three times and in triplicate.

Transmission Electron Microscopy. A549 lung epithelial cancer cells were grown in Dulbecco's Modified Eagle's Medium (DMEM) containing 10% fetal calf serum at 37 °C and in a 5% CO_2 atmosphere. The cells were trypsinised, counte, and adjusted to 100 000 cells mL^{-1} and 2 mL added per plate. Stock solutions of platinum-tethered nanoparticles were diluted using DMEM and added to the plate in 800 μL quantities. After incubation for 24 h, cells were thoroughly washed with phosphate-buffered saline (PBS) in order to eliminate nanoparticles that were not internalized. Cell processing for TEM analysis was carried out in situ, without displacement from the culture dish. Cells were fixed in a 0.1 M PBS solution containing 2.5% gluteraldehyde and 4% paraformaldehyde for 1 h. They were then rinsed with 0.1 M PBS and postfixed in 1% osmium tetroxide solution (***extremely toxic; use caution***) for 1 h, rinsed with distilled water, stained with 0.5% uranyl acetate for 1 h, dehydrated in a graded series of ethanol (30, 60, 70, 90, and 100%), and embedded in epoxy resin. The resin was polymerized at 60 °C for 48 h. Ultrathin sections (50−75 nm) obtained with an LKB ultramicrotome were stained with 2% aqueous uranyl acetate and 2% aqueous lead citrate and imaged under a 120 kV FEI Tecnai Spirit TEM.

In Vitro Growth Inhibition Assays. For the human lung cancer cell line A549 and the human colon cancer cell lines HCT116, HCT15, HT29, and RKO, cytotoxicity was determined by a tetrazolium dye-based microtitration assay.[27] Cells were grown in DMEM containing fetal calf serum (10%). Cells were plated out in 96-well plates at a density of 500−1000 cells per well and were allowed to attach and grow for 2 days. Cells were exposed to oxaliplatin, PEGylated gold nanoparticles, or platinum-tethered gold nanoparticles over a range of concentration for 72 h, and then the medium was replaced with a drug-free medium for another 24 h. On the final day, MTT (50 μL of a 5 mg/mL solution) was added to the 200 μL of medium in each well, and the plates were incubated at 37 °C for 4 h in the dark. The medium and MTT were then removed, and the MTT-formazan crystals were dissolved in 200 μL of DMSO. Glycine buffer (25 μL per well, 0.1 M, pH 10.5) was added, and the absorbance was measured at 570 nm in a multiwell plate reader. A typical dose−response curve consisted of eight drug concentrations, and two wells were used per drug concentration.

Drug Uptake. A549 cells were plated out at a density of 10^6 cells per well in six well plates and incubated overnight at 37 °C

(10) Wilton-Ely, J. D. E. T. *Dalton Trans.* **2008**, 25.
(11) McKenzie, F.; Faulds, K.; Graham, D. *Chem. Commun.* **2008**, 2367.
(12) Eck, W.; Craig, G.; Sigdel, A.; Gerd, R.; Old, L. J.; Tang, L.; Brennan, M. F.; Allen, P. J.; Mason, M. D. *ACS Nano* **2008**, *2*, 2263.
(13) Connor, E. E.; Mwamuka, J.; Gole, A.; Murphy, C. J.; Wyatt, M. D. *Small* **2005**, *1*, 325.
(14) Male, K. B.; Lachance, B.; Hrapovic, S.; Sunahara, G.; Luong, J. H. T. *Anal. Chem.* **2008**, *80*, 5487.
(15) Ghosh, P. S.; Kim, C.-K.; Han, G.; Forbes, N. S.; Rotello, V. M. *ACS Nano* **2008**, *2*, 2213.
(16) Cheng, Y.; Samia, A. C.; Meyers, J. D.; Panagopoulos, I.; Fei, B.; Burda, C. *J. Am. Chem. Soc.* **2008**, *130*, 10643.
(17) Hauck, T. S.; Jennings, T. L.; Yatsenko, T.; Kumaradas, J. C.; Chan, W. C. W. *Adv. Mater.* **2008**, *20*, 3832.
(18) Au, L.; Zheng, D.; Zhou, F.; Li, Z.-Y.; Li, X.; Xia, Y. *ACS Nano* **2008**, *2*, 1645.
(19) Dhar, S.; Daniel, W. L.; Giljohann, D. A.; Mirkin, C. A.; Lippard, S. J. *J. Am. Chem. Soc.* **2009**, *131*, 14652.
(20) www.cytimmune.com.
(21) Turkevich, J. *Gold Bull.* **1985**, *18*, 86.
(22) Grabar, K. C.; Brown, K. R.; Keating, C. D.; Stranick, S. J.; Tang, L. S.; Natan, M. *J. Anal. Chem.* **1997**, *69*, 471.
(23) Grabar, K. C.; Freeman, R. G.; Hommer, M. B.; Natan, M. *J. Anal. Chem.* **1995**, *67*, 735.
(24) Jana, N. R.; Gearheart, L.; Murphy, C. J. *Chem. Mater.* **2001**, *13*, 2313.
(25) Meltzer, S.; Pesch, R.; Koel, B. E.; Thompson, M. E.; Madhukar, A.; Requicha, A. A. G.; Will, P. *Langmuir* **2001**, *17*, 1713.
(26) Sau, T. K.; Pal, A.; Jana, N. R.; Wang, Z. L.; Pal, T. *J. Nanopart. Res.* **2001**, *3*, 257.
(27) Plumb, J. A.; Milroy, R.; Kaye, S. B. *Cancer Res.* **1989**, *49*, 4435.

in a humidified atmosphere of 10% CO_2 in air. The medium was then replaced with fresh medium alone or with medium containing oxaliplatin or platinum-tethered gold nanoparticles for 4 h. The medium was removed, and the cells were then washed with ice-cold PBS and lysed by the addition of 215 μL of nitric acid (OPTIMA 68%) to each well. The cells were then collected in an eppendorf tube and incubated overnight at 65 °C. They were then diluted with water/0.1% Triton-X100 to a final concentration of 1% acid before the platinum content of the samples was determined by ICP-MS. Uptake is expressed as nanograms of platinum per 10^6 cells.

Synthesis of Naked Gold Nanoparticles. $NaAuCl_4 \cdot 2H_2O$ (50 mg, 0.14 mmol) was dissolved in distilled water (500 mL) and heated to 100 °C with continuous stirring. Upon boiling, sodium citrate (1% m/v, 7.5 mL) was added, and the solution boiled for 15 min before cooling to room temperature. UV−visible spectra (λ_{max} = 519−523 nm) indicated the successful formation of the colloid.

Synthesis of PEG Linker. Wang resin (0.5 g, 1 mmol/g loading) was suspended in DCM (50 mL). To this, succinic anhydride (0.25 g, 5 equiv) and dimethylaminopyridine (0.3 g, 5 equiv) were added. This was then refluxed at 60 °C for 6 h. The resin was separated from the mixture by filtration and washed several times with DCM and MeOH. The acid functionalization of the resin was tested with malachite green. The resin was then resuspended in DCM (50 mL). Jeffamine ED-2003 (4.25 g, 5 equiv) and *N*,*N*-diisopropylcarbodiimide (387 μL, 5 equiv) were added, and the mixture was shaken overnight. The resin was then separated from the mixture as before, using filtration, and was washed several times with copious amounts of DCM and MeOH. The resin was once again suspended in DCM (50 mL), and to this *N*,*N*-diisopropylcarbodiimide (387 μL, 5 equiv) and thioctic acid (0.516 g, 5 equiv) were added. The mixture was shaken overnight in the absence of light and then washed as before with DCM and MeOH. The resin was suspended in 10% trifluoroacetic acid in DCM at room temperature for 3 h and shaken to cleave the desired compound. The resin was removed by filtration, and the filtrate was concentrated under reduced pressure. The remaining liquid was then washed with diethylether, which was subsequently decanted, and the product was left to dry under high vacuum overnight. Yield: 386 mg, 18%.

Assembly of Platinum-Tethered Nanoparticles. To an eppendorf tube containing gold nanoparticles (1 mL, 17 nM) was added PEG linker (100 μL, 1 mM), and the solution was allowed to form a monolayer on the nanoparticles by shaking for 4 h. To wash away unbound PEG linker, the nanoparticles were centrifuged at 7000 rpm for 20 min, the supernatant was removed, and the remaining pellet was dissolved in Milli-Q water (1 mL). This was repeated once more. *N*,*N*-Diisopropylethylamine (100 μL, 0.1 mM) was added to the nanoparticles. [Pt(*R*,*R*-dach)$(H_2O)_2$]$2NO_3$[28] (10 mg) was dissolved in 1,3-dimethyl-3,4,5,6-tetrahydro-2(1*H*)-pyrimidone (1 mL), added to the nanoparticles in 10−100 μL aliquots, and left overnight. Finally, the gold nanoparticles were centrifuged, the supernatant was removed, the remaining pellet was resuspended in Milli-Q water (1 mL), and the wash was repeated once more.

Results and Discussion

Nanoparticle Synthesis. The production of the platinum-tethered nanoparticles began with the synthesis of citrate-reduced gold nanoparticles from sodium tetrachloroaurate(III) dihydrate (Figure 1). The attachment of [Pt(*R*,*R*-dach)] then required the design, synthesis, and attachment of a suitable linker. Alkyl thiol−gold chemistry has been well established in terms of functionalizing gold surfaces and nanoparticles to form stable monolayers;[29] however, these are normally hydrophobic in nature and, as such, are not ideal for biological applications. In addition, the thiol−gold bond is susceptible to displacement by strong nucleophiles commonly found in vivo.[30] To overcome this, we used a cyclic disulfide to bind the linker to the nanoparticles. In the past, this has increased the stability to such an extent that displacement by millimolar concentrations of dithiothreitol (an unusually strong reducing agent) was not possible.[31,32] Additionally, our monolayer also contains a stabilizing linkage that is hydrophobic on the inner core of the nanoparticle but then converts to being hydrophilic on the outer part of the sphere to make it compatible with a biological environment (e.g., use of polyethylene glycol (PEG) spacers). The PEG linker used on our nanoparticles in this study was made using solid-phase synthesis beginning with refluxing succinic anhydride with Wang resin to yield a carboxylic acid group available for amide formation with a bis-amino PEG copolymer (Figure 1). One amine group of the copolymer was coupled to the carboxylic acid on the resin, and the other was reacted with thioctic acid. Washing away unbound reagents from the resin in between each step and cleavage with trifluoroacetic acid yielded a PEG linker with an average molecular weight of 2080 g mol^{-1}.

The formation of a PEG monolayer on the surfaces of the gold nanoparticles was achieved through shaking in water, with excess linker removed by centrifugation. The active component of oxaliplatin, [Pt(*R*,*R*-dach)], was then added to the surface of the PEGylated nanoparticles (Figure 1). Unbound platinum was removed by centrifugation, yielding a dark-red solution.

Nanoparticle Characterization. The platinum-tethered gold nanoparticles were characterized by electron probe microanalysis (EPMA) to confirm that both gold and platinum were present through their elemental peaks at 2.12 and 2.05 keV, respectively (Figure 2). Although the amounts of gold and platinum in the sample could not be determined quantitatively because of scattering effects from the rough surfaces of the nanoparticles, the spectra clearly indicated that each nanoparticle contained a much larger percentage of gold compared to platinum. The number of [Pt(*R*,*R*-dach)] molecules per gold nanoparticle, after digestion with sodium cyanide, was determined to be 280 (±20) by ICP-MS. This represents a significant improvement in the number of drug molecules that can be carried on other delivery scaffolds, such as carbon nanotubes (82 drug molecules per NT),[33] hyperbranched polymers (3−6 drug molecules),[34] or dendrimers (30−104 depending on the dendrimer generation/size).[35,36] It is possible that our gold nanoparticles could be made to deliver even more drug molecules if other linker terminal groups, such as bidentate carboxylates, are used to couple the platinum molecules more strongly to the nanoparticle.

The size and charge of the naked gold nanoparticles, the PEGylated nanoparticles, and the platinum-tethered nanoparticles were determined by dynamic light scattering (Table 1).

(28) Wheate, N. J.; Taleb, R. I.; Krause-Heuer, A. M.; Cook, R. L.; Wang, S.; Higgins, V. J.; Aldrich-Wright, J. R. *Dalton Trans.* **2007**, 5055.
(29) Brust, M.; Walker, M.; Bethell, D.; Schiffrin, D. J.; Whyman, R. *J. Chem. Soc., Chem. Commun.* **1994**, 801.
(30) Zhang, G., Y. Z.; Lu, W.; Zhang, R.; Huang, Q.; Tian, M.; Li, L.; Liang, D.; Li, C *Biomaterials* **2009**, *30*, 1928.
(31) Li, Z.; Mirkin, C. A.; Letsinger, R. L. *Nucleic Acids Res.* **2002**, *30*, 1558.
(32) Dougan, J. A.; Karlsson, C.; Smith, W. E.; Graham, D. *Nucleic Acids Res.* **2007**, *35*, 3668.
(33) Dhar, S.; Liu, Z.; Thomale, J.; Dai, H.; Lippard, S. J. *J. Am. Chem. Soc.* **2008**, *130*, 11467.
(34) Haxton, K. J.; Burt, H. M. *Dalton Trans.* **2008**, 5872.
(35) Howell, B. A.; Fan, D.; Rakesh, L. *J. Therm. Anal. Calor.* **2006**, *85*, 17.
(36) Pisani, M. J.; Wheate, N. J.; Keene, F. R.; Aldrich-Wright, J. R.; Collins, J. G. *J. Inorg. Biochem.* **2009**, *103*, 373.

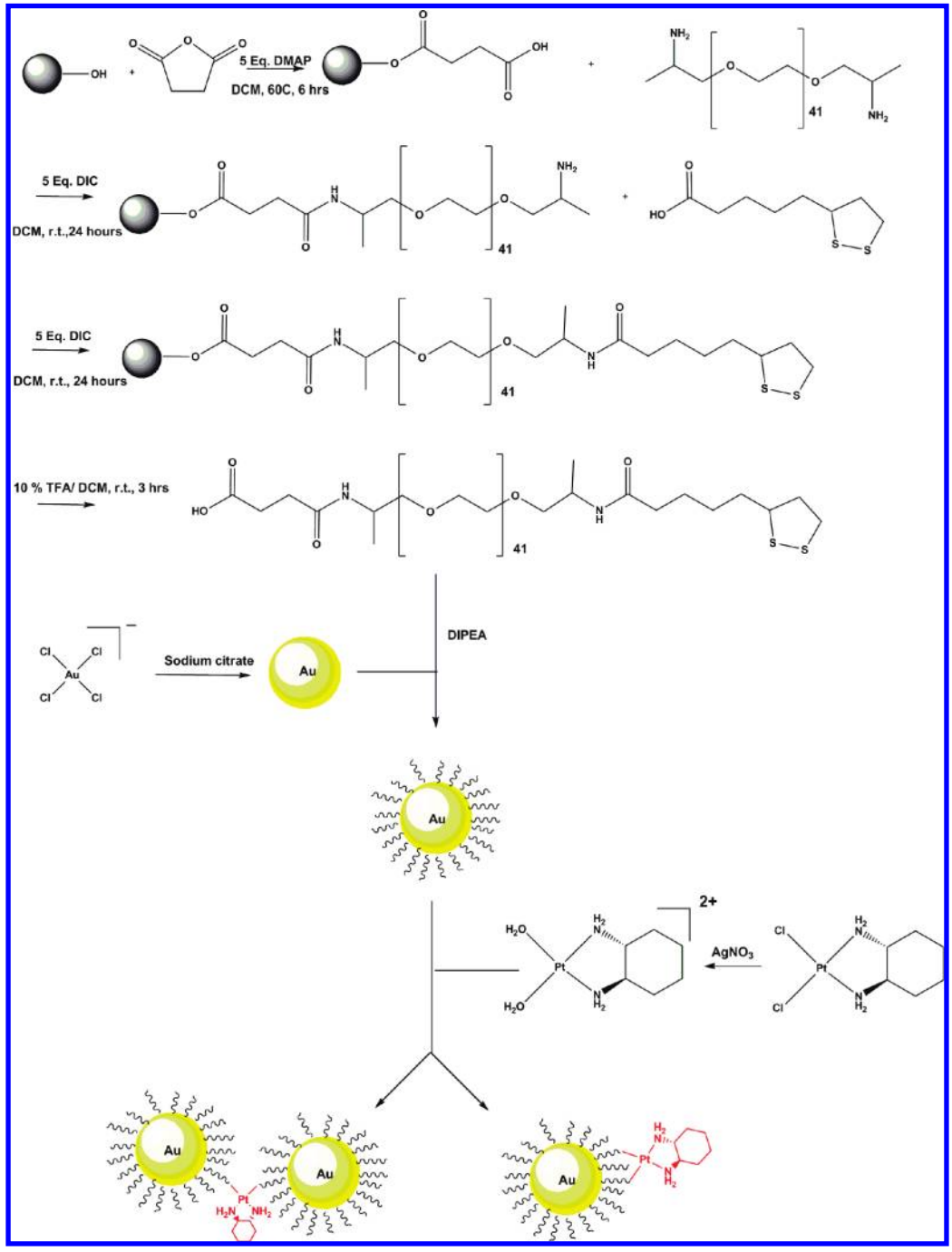

Figure 1. Chemical synthesis of the platinum-tethered gold nanoparticles.

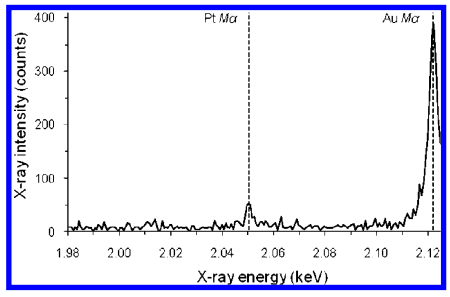

Figure 2. Electron probe microanalysis spectrum of platinum-tethered gold nanoparticles showing the presence of gold (2.12 eV) and platinum (2.05 eV) in the sample.

Upon addition of the PEG linker, the nanoparticles increase in size slightly but maintain a similar zeta potential because of the negative charge of the terminal carboxylate groups. Upon addition of [Pt(*R*,*R*-dach)], the nanoparticles increase significantly in size (4.5-fold) and change from a net negative to a positive charge. This increase was unexpected and is thought to represent either aggregation of the nanoparticles through hydrophobic interactions between the cyclohexane components of [Pt(*R*,*R*-dach)] or the cross linking of multiple nanoparticles using [Pt(*R*,*R*-dach)] as a bridging ligand (Figure 1). This increase in size might be a potential problem when using these nanoparticles in vivo, and methods to prevent the aggregation of platinum-tethered gold nanoparticles may therefore need to

Table 1. Zeta Potential and Particle Size of the Naked Gold Nanoparticles, PEGylated Nanoparticles, PEGylated Nanoparticles with Added Diisopropylethylamine (DIPEA) Base to Deprotonate the Carboxylic Acid Groups, and the Platinum-Tethered Nanoparticles, as Determined by Dynamic Light Scattering

nanoparticle	zeta potential (mV)	diameter (nm)
naked nanoparticle	-27.7 ± 0.7	31 ± 1.2
PEGylated nanoparticle	-24.4 ± 5.2	38.5 ± 0.1
PEGylated nanoparticle + DIPEA	-28.4 ± 8.9	40.6 ± 1.4
platinum-tethered nanoparticle	$+14 \pm 7.0$	176 ± 25

be developed. Research by Maeda et al. on the enhanced permeability and retention effect in tumors, however, has shown that the vasculature of solid cancers leaves them susceptible to nanoscale-sized particles.[37] Typically, tumors have intercellular spaces of between 100 and 1200 nm.[5] Recent research has shown that nanoparticles with diameters of less than 200 nm are ideal for targeting tumors,[38] which means that the aggregation seen for our platinum-tethered gold nanoparticles, rather than being a problem, may even be beneficial and assist them in being more selective for solid cancers.

The size and aggregation of the platinum-tethered nanoparticles was further examined by scanning electron microscopy (Figure 3). The naked nanoparticles are approximately 21−29 nm in diameter, and the PEGylated nanoparticles are roughly 30−40 nm, with some evidence of aggregation. The platinum-tethered nanoparticles appear to be approximately the same diameter as the PEGylated nanoparticles but are now more aggregated. Because of the drying nature of the technique, it is impossible to calculate the degree of aggregation or whether this aggregation is due to [Pt(*R*,*R*-dach)] molecules bridging multiple nanoparticles or simply is due to hydrophobic interactions.

In Vitro Cytotoxicity. Lung and colorectal cancers are the first and third most common cancer types in the world, respectively.[39] As such, the ability of the nanoparticles to induce cellular apoptosis was determined using growth-inhibition assays with the A549 human lung epithelial and the HCT116, HCT15, HT29, and RKO human colon cancer cell lines. The PEGylated nanoparticles demonstrated no cytotoxicity at concentrations up to 10 nM in all five cancer cell lines (Table 2). In contrast, the platinum-tethered gold nanoparticles had an IC_{50} of 0.495 nM in the A549 cell line (based on the gold nanoparticle concentration; 0.135 μM based on the number of [Pt(*R*,*R*-dach)] molecules per nanoparticle), which is almost 6-fold more active than oxaliplatin ($IC_{50} = 0.775$ μM). In the colon cancer cell lines, the platinum-tethered gold nanoparticles are up to 5.6-fold more cytotoxic or at least as active as oxaliplatin (Table 2).

It was originally thought that the benefit of the platinum-tethered gold nanoparticles would be from their enhanced plasma retention and circular times and better uptake into solid tumors, in vivo, compared with cisplatin. Therefore, the enhanced in vitro cytotoxicity was unexpected and suggests that gold nanoparticle-based delivery of platinum drugs may significantly improve their potency, possibly through enhanced cellular uptake. Importantly, our nanoparticles do not rely on near-infrared radiation to induce their cytotoxic effect, as many gold nanoparticle drug-delivery systems do,[16−18,40] thus greatly simplifying their application in treating cancer.

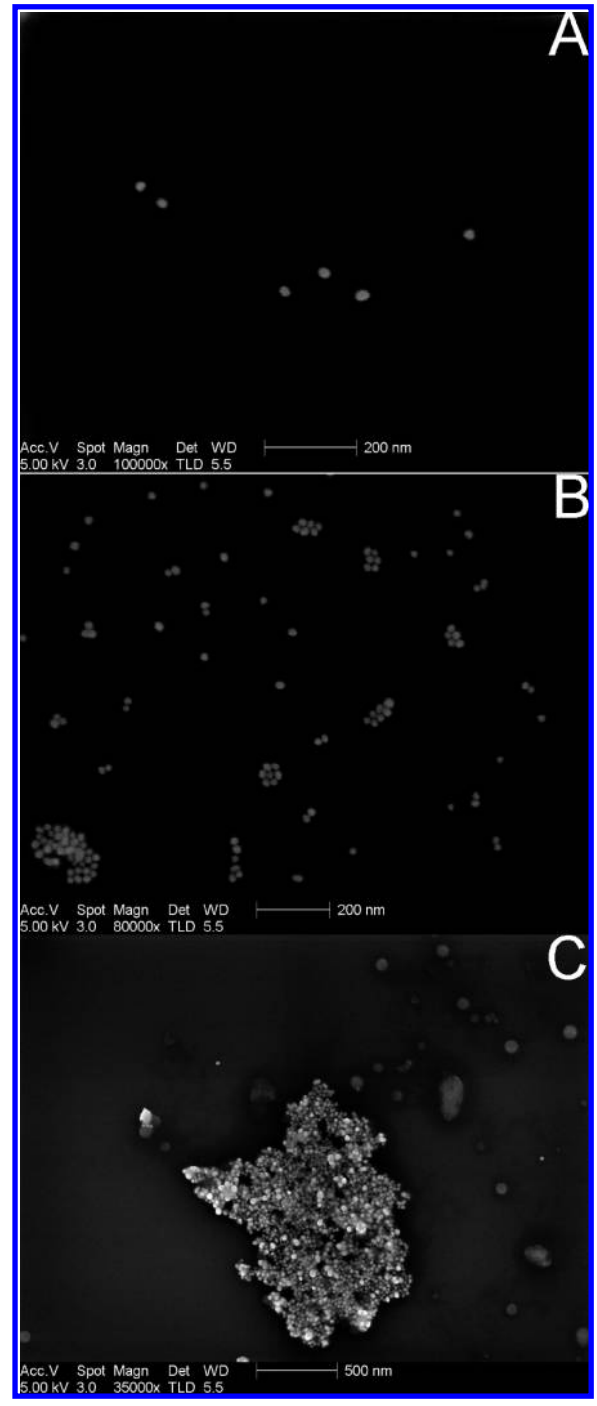

Figure 3. Scanning electron microscope pictures of (A) naked gold nanoparticles, (B) gold nanoparticles with a monolayer of PEG linker, and (C) platinum-tethered gold nanoparticles, showing their increase in size with functionalization and the high propensity of the platinum-tethered nanoparticles to aggregate in both the solution and solid state.

Cellular Uptake and Localization. Given the excellent cytotoxicity, the uptake and localization of the platinum-tethered nanoparticles were then examined using ICP-MS and transmission electron microscopy. A549 lung cancer cells were incubated with oxaliplatin and platinum-tethered gold nanoparticles at equal [Pt(*R*,*R*-dach)] concentrations. After 4 h, the cells were

(37) Maeda, H.; Bharate, G. Y.; Daruwalla, J. *Eur. J. Pharm. Biopharm.* **2009**, *71*, 409.
(38) Gu, F. X.; Karnik, R.; Wang, A. Z.; Alexis, F.; Levy-Nissenbaum, E.; Hong, S.; Langer, R. S.; Farokhzad, O. C. *Nano Today* **2007**, *2*, 14.
(39) Wheate, N. J.; Collins, J. G. *Curr. Med. Chem.: Anti-Cancer Agents* **2005**, *5*, 267.
(40) Gil, P. R.; Parak, W. J. *ACS Nano* **2008**, *2*, 2200.

Table 2. Cytotoxicity of the PEGylated Gold Nanoparticles and the Platinum-Tethered Gold Nanoparticles in Colon Cancer Cell Lines HCT116, HCT15, HT29, and RKO and Human Lung Cancer Cell Line A549[a]

	IC_{50}				
		platinated nanoparticles			
cell line	PEGylated nanoparticles (nM)	wrt [Au] (nM)	wrt [Pt] (μM)	oxaliplatin control (μM)	fold increase
HCT116	>10	2.66 ± 0.27	0.734 ± 0.044	0.728 ± 0.048	1.0
HCT15	>10	2.36 ± 0.34	0.652 ± 0.093	2.97 ± 0.21	4.6
HT29	>10	1.29 ± 0.03	0.357 ± 0.007	2.00 ± 0.15	5.6
RKO	>10	0.842 ± 0.127	0.233 ± 0.035	0.295 ± 0.021	1.3
A549	>10	0.495 ± 0.062	0.135 ± 0.008	0.775 ± 0.057	5.7

[a] The cytotoxicity of the platinum-tethered gold nanoparticles is given in terms of both the concentration of gold nanoparticles and as the platinum drug concentration. The fold increase is the cytotoxicity of the platinum-tethered nanoparticles (with respect to the concentration of platinum) in relation to oxaliplatin itself.

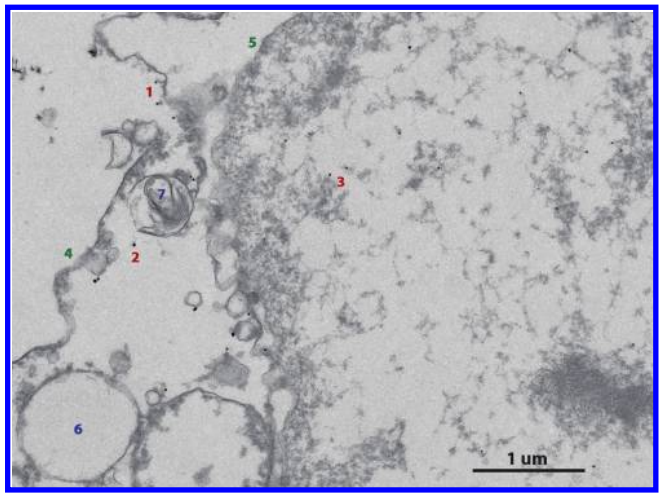

Figure 4. Section of a whole cell transmission electron microscope image showing both the intracellular and intranuclear uptake of the platinum-tethered gold nanoparticles into A549 lung cancer cells: (1) extracellular nanoparticles, (2) intracellular nanoparticles, (3) intranuclear nanoparticles, (4) contracted cell wall, (5) double-envelope nuclear membrane, (6) endosome, and (7) lysosome.

washed and digested, and the platinum content was determined. The results demonstrate a significantly higher uptake of [Pt(*R*,*R*-dach)] by the gold nanoparticles inside the cell (21.34 ± 0.89 ng Pt/10^6 cells) compared with that of oxaliplatin (10.19 ± 0.95 ng Pt/10^6 cells) and also demonstrate that the gold nanoparticles are capable of delivering [Pt(*R*,*R*-dach)] to the cell and then releasing it.

The A549 lung cells were also incubated with 225 nM platinum-tethered nanoparticles for 24 h, and the uptake was examined using transmission electron microscopy (TEM). The resultant images show a number of important features, particularly intracellular accumulation of the gold nanoparticles (Figure 4). At the nanoparticle concentration tested, cell growth was very significantly hindered and cell stress is seen by a large contraction of the cell wall toward the nucleus. Gold nanoparticles are observed both inside and in contact with the plasma membrane of the cell but more importantly also within the cell nucleus. Nonfunctionalized gold nanoparticles are known not to be able to penetrate cell nuclei,[41] and neither the naked nanoparticles nor the PEGylated nanoparticles when tested under the same conditions as the platinum-tethered nanoparticles are observed in the nucleus. This result implies some sort of [Pt(*R*,*R*-dach)]-mediated transport mechanism into the nucleus, where presumably the drug is then released to bind with DNA.

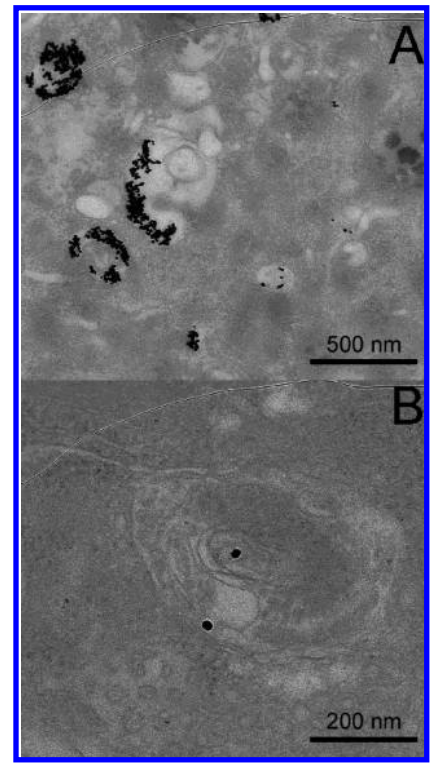

Figure 5. TEM images of A549 lung cancer cells showing (A) endocytosis of naked gold nanoparticles into the cell and (B) PEGylated gold nanoparticles.

The uptake of gold nanoparticles into mammalian cells and macrophages is usually via endocytosis.[41−43] Whereas both endosomes and lysosomes are observed in the TEM images, no platinum-tethered nanoparticles are located within them. Conversely, both the naked and PEGylated nanoparticles demonstrated cellular uptake through endocytosis (Figure 5). Previously, some cationic nanoparticles have been shown to enter cells by generating transient holes in the membrane,[41] and it is possible that our platinum-tethered nanoparticles are taken up by the cancer cells in a similar manner. Interestingly, the previously observed aggregation of the nanoparticles was not observed and did not appear to inhibit uptake. The reason for the lack of aggregation is unclear but may be due to the lower concentration of the nanoparticles or because [Pt(*R*,*R*-dach)] had

(41) Verma, A.; Uzun, O.; Hu, Y.; Hu, Y.; Han, H.-S.; Watson, N.; Chen, S.; Irvine, D. J.; Stellacci, F. *Nat. Mater.* **2008**, *7*, 588.
(42) Stokes, R. J.; McKenzie, F.; McFarlane, E.; Ricketts, A.; Tetley, L.; Faulds, K.; Alexander, J.; Graham, D. *Analyst* **2009**, *134*, 170.
(43) Schneider, G. F.; Subr, V.; Ulbrich, K.; Decher, G. *Nano Lett.* **2009**, *9*, 636.

already been released and thus was not acting as a bridging ligand between two individual nanoparticles.

Conclusions

In this article, we have developed a drug-delivery strategy for platinum-based anticancer drugs based on gold nanoparticles. The versatility of gold nanoparticles means that a large family of gold−platinum drug nanoparticles can now be produced to tune and improve the technology. This includes the synthesis of different sized gold particles (20−100 nm) on which to attach the drugs; linkers of different lengths and structure, including different terminal end groups such as dicarboxylates or even thiols; the use of different drugs including cisplatin and multinuclear drugs such as BBR3464;[39,44] and the attachment of active targeting groups such as folate and estrogen, prostate or leukemia targeting aptamers, lung cancer targeting peptides, or B-cell lymphoma targeting antibodies. This genuinely nanomedicine-based strategy offers a different approach to cancer therapy and holds significant potential to improve disease management and the treatment of cancer in the future.

Acknowledgment. This work was funded in part by a University of Strathclyde Research Development Grant (no. 1549).

JA908117A

(44) Wheate, N. J.; Collins, J. G. *Coord. Chem. Rev.* **2003**, *241*, 133.